

Spin dilution in frustrated two-dimensional $S = \frac{1}{2}$ antiferromagnets on a square lattice

N. Papinutto and P. Carretta

Department of Physics "A. Volta," University of Pavia, Via Bassi 6, I-27100, Pavia, Italy

S. Gonthier and P. Millet

CEMES, CNRS, Cedex, France

(Received 21 January 2005; published 26 May 2005)

^7Li and ^{29}Si nuclear magnetic resonance, muon spin relaxation (μSR), and magnetization measurements in $\text{Li}_2\text{V}_{1-x}\text{OTi}_x\text{SiO}_4$, for $0 \leq x \leq 0.2$, are presented. The $x=0$ compound is a prototype of frustrated two-dimensional Heisenberg antiferromagnet on a square-lattice with competing nearest- (J_1) and next-nearest- (J_2) neighbor exchange interactions. $\text{Ti}^{4+}(S=0)$ for $\text{V}^{4+}(S=1/2)$ substitution yields the spin dilution of the antiferromagnetic layers. The analysis of the magnetization and of the nuclear spin-lattice relaxation rate shows that spin dilution not only reduces the spin stiffness by a factor $\approx (1-x)^2$, but also causes the decrease of the effective ratio $J_2(x)/J_1(x)$. Moreover, the sublattice magnetization curves derived from zero-field μSR measurements in the collinear phase point out that, at variance with nonfrustrated two-dimensional Heisenberg antiferromagnets, spin dilution affects the low-temperature staggered magnetization only to a minor extent. This observation is supported also by the x dependence of the collinear ordering temperature. The results obtained for the Ti doped samples are discussed in the light of the results previously obtained in the pure $x=0$ compound and in nonfrustrated two-dimensional Heisenberg antiferromagnets with spin dilution.

DOI: 10.1103/PhysRevB.71.174425

PACS number(s): 75.10.Jm, 76.60.-k, 76.75.+i

I. INTRODUCTION

The search for novel quantum states in low-dimensional antiferromagnets (AFs) has triggered a significant activity in recent times.¹ A remarkable amount of theoretical studies has concerned the phase diagram of antiferromagnets where long-range magnetic order is suppressed by enhanced quantum fluctuations. Such a scenario can be established when the magnetic lattice dimensionality and the spin value are reduced or when the disorder is increased, either by means of heterovalent substitutions or by spin dilution.²⁻⁴ Further enhancement of quantum fluctuations can occur when antiferromagnetic interactions are competing as, for instance, in frustrated two-dimensional $S=1/2$ Heisenberg AF (2DQHAF) on a square lattice, with nearest-neighbor (J_1) and next-nearest-neighbor (J_2) antiferromagnetic couplings of the same order of magnitude.⁵

Recently, a prototype of frustrated 2DQHAF on a square lattice has been discovered, $\text{Li}_2\text{VOSiO}_4$.⁶ The analysis of the magnetic susceptibility, of the specific heat and of other quantities⁷ indicate that this compound is characterized by a ratio J_2/J_1 ranging from 1 to 4.⁸ The ground state is collinear,^{6,9} as theoretically expected,¹⁰ and the staggered magnetization reaches a value $\approx 0.6\mu_B/V^{4+9}$, consistent with the J_2/J_1 estimate.¹¹ This value is remarkably close to the one of a nonfrustrated 2DQHAF (Ref. 12) and, therefore, at first sight one could think that, as far as J_2/J_1 is not close to 0.5 and quantum fluctuations are not so strong, frustration does not affect sizeably the static magnetic properties of a 2DQHAF. In order to unravel the basic differences in the properties of frustrated and nonfrustrated 2DQHAF it is tempting to compare also the behavior of these systems when disorder is introduced, for example, by spin dilution. Spin dilution has been widely investigated in prototypes of non-

frustrated 2DQHAF, as $\text{La}_2\text{Cu}_{1-x}(\text{Zn}, \text{Mg})_x\text{O}_4$,^{4,13-15} and evidence for the validity of the simple dilution model with a renormalization of the spin stiffness and for the disappearance of long-range magnetic order at the classical percolation threshold has been given.^{4,14} At first, in a frustrated 2DQHAF on a square lattice one would expect that the enhancement of quantum fluctuations leads to a suppression of the long-range order well below the percolation threshold. However, one should also consider that, owing to the next-nearest-neighbor coupling, the percolation threshold extends to much larger doping levels with respect to nonfrustrated antiferromagnets.¹⁶ Hence, it is not trivial to say *a priori* how the magnetic properties vary upon increasing the spin dilution.

In the following an experimental study of spin dilution effects in frustrated 2DQHAF on a square lattice will be presented. In $\text{Li}_2\text{VOSiO}_4$ spin dilution can be achieved upon $\text{Ti}^{4+}(S=0)$ for $\text{V}^{4+}(S=1/2)$ substitution. It is found that spin dilution not only reduces the spin stiffness by a factor $\approx (1-x)^2$, but also causes a reduction of the effective ratio $J_2(x)/J_1(x)$. The analysis of the sublattice magnetization curves shows that, at variance with nonfrustrated 2DQHAF, spin dilution affects the low-temperature staggered magnetization only to a minor extent. The x dependence of the collinear ordering temperature and of other quantities will be discussed vis-à-vis with the trend observed for nonfrustrated 2DQHAF. In the following section a description of the technical aspects involved in the sample preparation, magnetization, nuclear magnetic resonance (NMR), and muon spin relaxation (μSR) measurements will be presented together with the experimental data. Then the results will be discussed in the light of models which turned out to be valid for nonfrustrated spin-diluted 2DQHAF. The final conclusions will be given in Sec. IV.

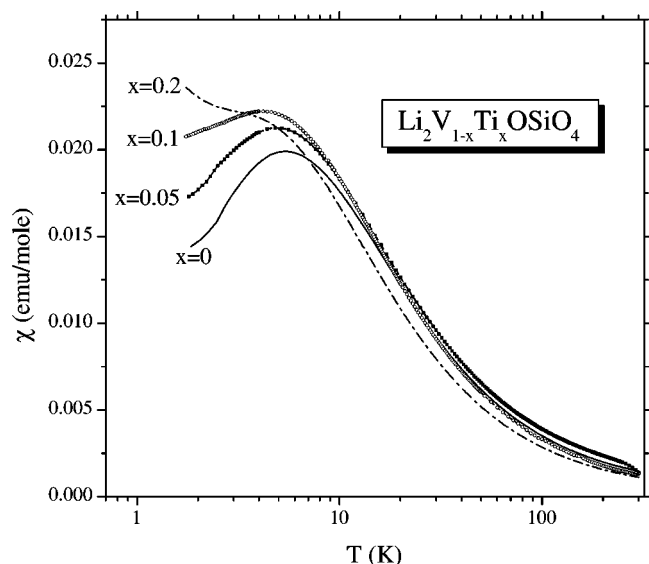


FIG. 1. Temperature dependence of the susceptibility in $\text{Li}_2\text{V}_{1-x}\text{Ti}_x\text{OSiO}_4$ for different Ti contents, in a magnetic field of 1 kG.

II. TECHNICAL ASPECTS AND EXPERIMENTAL RESULTS

A. Sample preparation and magnetization measurements

Powder samples of $\text{Li}_2\text{V}_{1-x}\text{Ti}_x\text{OSiO}_4$ were prepared in a platinum crucible by solid state reaction starting from a stoichiometric mixture of Li_2SiO_3 (Aldrich, 99.5%), TiO_2 (Aldrich, 99.8%), and VO_2 at 830 °C, under vacuum, for 24 h.¹⁷ VO_2 was prepared from a stoichiometric mixture of V_2O_5 and V_2O_3 by heating in a vacuum-sealed quartz tube at 650 °C for 24 h. V_2O_3 itself was obtained by reducing V_2O_5 (99.9%, Aldrich Chem., Co.) under hydrogen at 800 °C. The sample purity was analyzed by means of x-ray powder diffraction and all peaks corresponded to the ones of $\text{Li}_2\text{VOSiO}_4$. The lattice parameters of each sample were refined using the program CELREF. The substitution of Ti for V leads to no significative variation of the cell parameters, which is consistent with the rather similar ionic radii of the two ions [$r_V=0.53$ Å and $r_{Ti}=0.51$ Å (Ref. 18)]. Upon varying x from 0 to 0.15 the a axes varies from 6.3683(4) Å to 6.3678(6) Å while the c axes varies from 4.449(3) Å to 4.4502(4) Å. The homogeneity of Ti concentration in the different samples was verified by EDX (energy dispersive x-ray analysis).

Magnetization measurements on $\text{Li}_2\text{V}_{1-x}\text{Ti}_x\text{OSiO}_4$ powders were performed using a Quantum Design XPMS-XL7 SQUID magnetometer. The temperature dependence of the susceptibility, defined as $\chi=M/H$ is shown in Fig. 1. One observes a high-temperature Curie-Weiss behavior, a low-temperature maximum indicating the onset of antiferromagnetic correlations and a small kink in the 2–3 K range signaling a phase transition to a collinear ground state. In the more doped sample, with 20% of Ti, a low-temperature upturn is noticed. This upturn is typical of diluted 2DQHAF (Ref. 19) and originates from the correlated response of the spins around the $S=0$ impurity. Above 20 K the data can be conveniently fitted according to

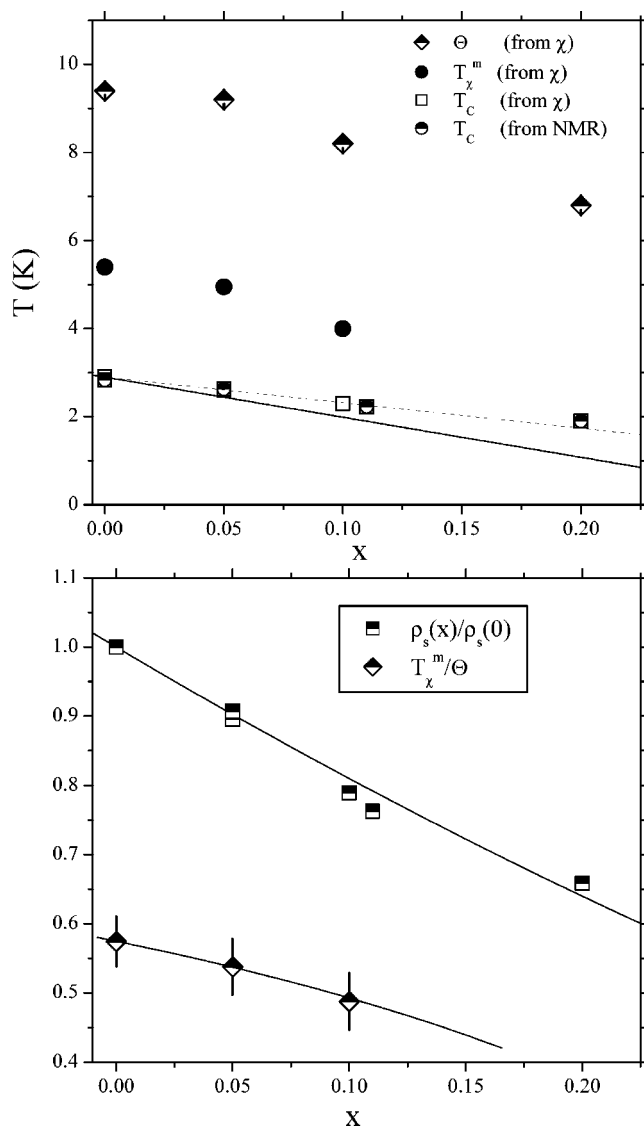


FIG. 2. (Top) Doping dependence of T_χ^m , Θ , and T_c as derived from susceptibility and NMR measurements. Lines track the initial suppression relation $-dT_c(x)/dx=CT_c(0)$ described in the text, with $C=3.2$ (solid line) and $C=2$ (dotted line). (Bottom) The spin stiffness $\rho_s(x)$, derived from Eq. (5) (see text), and the ratio $T_\chi^m(x)/\Theta(x)$ are reported for different Ti contents. The solid line passing through $\rho_s(x)/\rho_s(0)$ data is the function $(1-x)^2$. The one through $T_\chi^m(x)/\Theta(x)$ points is a guide to the eye.

$$\chi = \frac{C}{T + \Theta} + \chi_{VV}, \quad (1)$$

where C is Curie constant, Θ the Curie-Weiss temperature, and $\chi_{VV}=4 \times 10^{-4}$ emu/mole⁶ the T -independent Van-Vleck susceptibility.⁶ The x dependence of the Curie-Weiss temperature is shown in Fig. 2, together with the x dependence of the temperature T_χ^m at which χ displays a maximum and of the transition temperature T_c to the collinear phase. This latter quantity was estimated from the peak in the derivative $d\chi/dT$. One notices basically a monotonous decrease of all three quantities with increasing dilution, as expected.

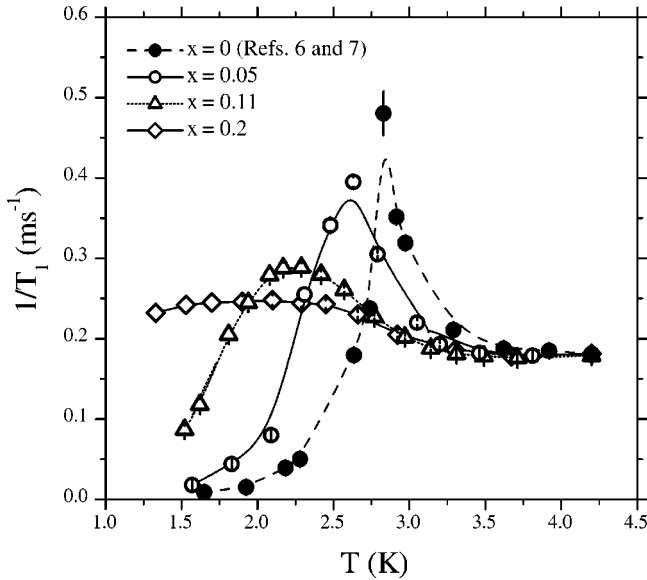


FIG. 3. Temperature dependence of ${}^7\text{Li}$ nuclear spin-lattice relaxation rate in $\text{Li}_2\text{V}_{1-x}\text{OTi}_x\text{SiO}_4$ powders for different doping amounts x . The $x=0$ data (Refs. 6 and 7) were measured on a single crystal with $\vec{H}\parallel c$. In order to compare them with the powder sample data they were divided by a factor 1.18 owing to the different hyperfine coupling involved. The lines are guide to the eye.

B. NMR measurements

${}^7\text{Li}$ and ${}^{29}\text{Si}$ NMR measurements have been carried out using standard radio frequency pulse sequences. In particular, the nuclear spin-lattice relaxation rate $1/T_1$ was estimated from the recovery of the nuclear magnetization after a saturating pulse sequence. Since in the powder sample at low- T ${}^7\text{Li}$ NMR line broadens due to the paramagnetic shift anisotropy, only a partial irradiation of the central and satellite lines is achieved. This causes a departure of the recovery law from a single exponential and hence at low temperature, below about 3 K, it is more convenient to fit the recovery of the nuclear magnetization with a stretched exponential form, namely $M(\tau) = M(\infty)\{1 - \exp[-(\tau/T_1)^\beta]\}$. The exponent β decreased down to $\beta \approx 0.7$ for $T \approx 1.3$ K. On the other hand, the recovery law for ${}^{29}\text{Si}$ was a single exponential over all the explored T range. The temperature dependence of ${}^7\text{Li}$ and ${}^{29}\text{Si}$ $1/T_1$ derived from the fit of the recovery laws following the aforementioned procedure are shown in Figs. 3 and 4, respectively. One notices that while ${}^7\text{Li}$ $1/T_1$ displays a peak at T_c , which broadens upon increasing x , ${}^{29}\text{Si}$ $1/T_1$ does not show any peak and the relaxation rate is found to decrease on cooling.

C. μSR measurements

μSR measurements were performed on the EMU instrument at the ISIS pulsed muon facility, using 29 MeV/ c spin-polarized muons. $\text{Li}_2\text{V}_{1-x}\text{Ti}_x\text{OSiO}_4$ powders were pressed on a silver sample-holder, whose background contribution to the muon asymmetry was determined from the slowly decaying oscillating signal in a 100 G transverse magnetic field, below T_c . In fact, below T_c the external magnetic field sums up with

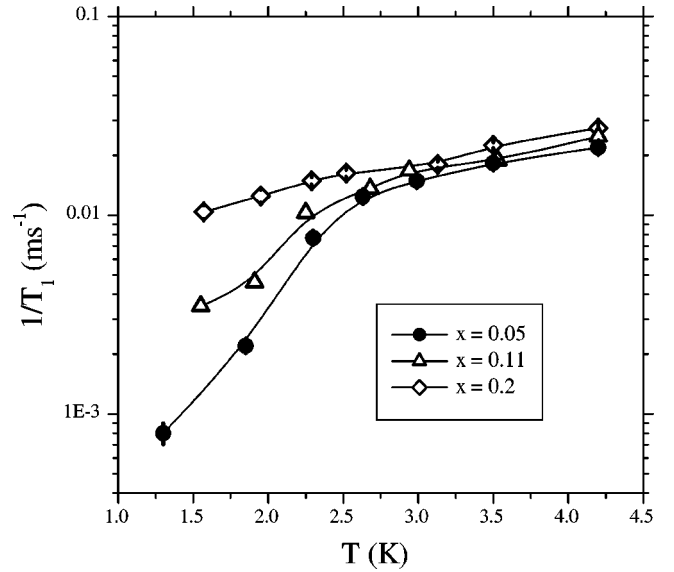


FIG. 4. Temperature dependence of ${}^{29}\text{Si}$ nuclear spin-lattice relaxation rate in $\text{Li}_2\text{V}_{1-x}\text{OTi}_x\text{SiO}_4$ for different doping amounts x . The lines are guide to the eye.

the randomly oriented internal field H_{int} and gives rise to a fast damping of the oscillating signal due to the muons stopping in the sample. The background was estimated $A_{\text{back}} \approx 0.071$ for $x=0.05$ and $A_{\text{back}}=0.0475$ for $x=0.11$. These values were kept fixed for all the subsequent fits.

By means of zero field (ZF) muon spin relaxation measurements it is possible to extract the temperature dependence of the order parameter below T_c , as previously done for the pure $\text{Li}_2\text{VOSiO}_4$.²⁰ Below T_c , superposed to an almost constant background, one observes a precessional signal at frequency $\omega_\mu = \gamma_\mu H_{\text{int}}$ (Fig. 5), with γ_μ the muon gyromagnetic ratio and H_{int} the local magnetic field at the muon generated by the collinear order. In a powder about 2/3 of the total signal oscillates while about 1/3 of the muons are in a longitudinal field configuration. Hence, one can write for the decay of the muon asymmetry

$$A(t) = A_T \cos(\gamma_\mu H_{\text{int}} t + \phi_0) \exp(-\sigma t) + A_L \exp(-\lambda t) + A_{\text{back}} \quad (2)$$

with A_T the asymmetry of the oscillating component and A_L the one of the longitudinal component. The ratio A_T/A_L deviates from 2 and is T dependent since at a pulsed muon source the amplitude of the oscillating part is progressively filtered out as the precessional frequency increases. The reduction in A_T on cooling is actually slightly more pronounced than what one would expect, taking into account that at ISIS the width of the muon pulse is about 70 ns. This suggests that a small part (a fraction below 15%) of the initial asymmetry is lost due to fast relaxing muons. This observation is supported by preliminary experiments performed at PSI facility. There it was found that the asymmetry decay is characterized by a certain distribution of relaxation rates, typical of systems with impurities, and that a fraction of muons relax too fast to be detected at ISIS pulsed muon facility. In Fig. 6 the T dependence of H_{int} for $x=0.05$ is

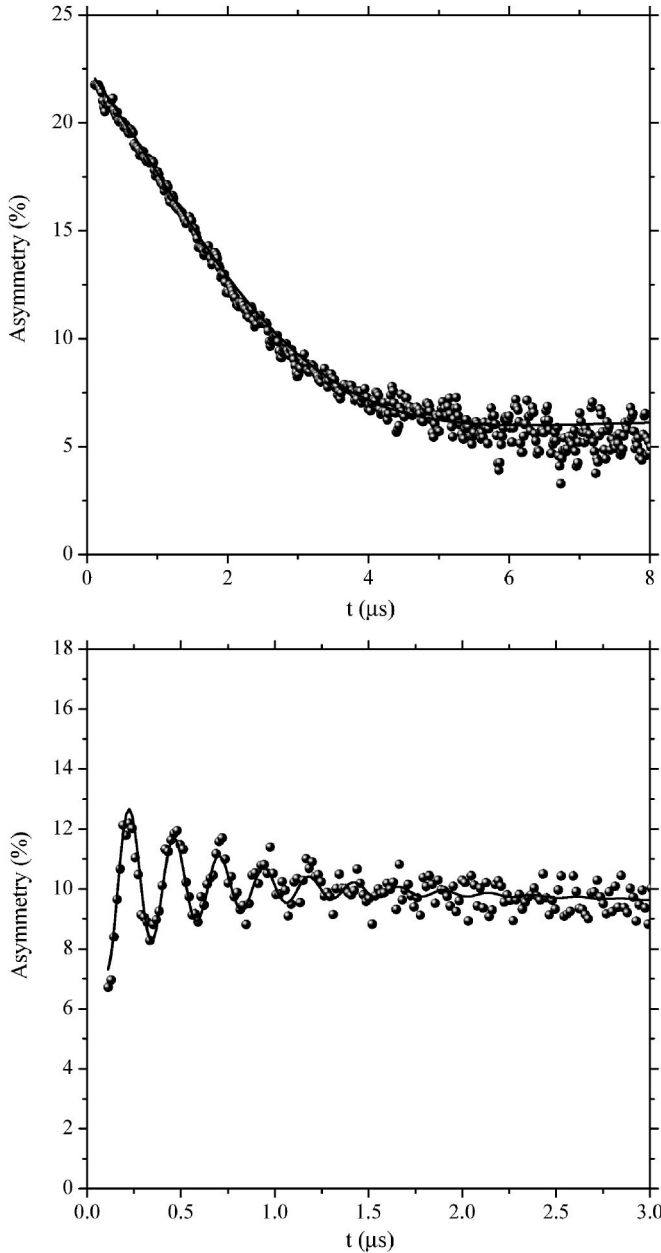


FIG. 5. μ SR asymmetry in $\text{Li}_2\text{V}_{1-x}\text{OTi}_x\text{SiO}_4$ for $x=0.05$ at 2.8 K (top) and 0.5 K (bottom). The solid line in the lower plot is the fit according to Eq. (2) in the text, while the one in the upper plot is the fit according to Eq. (3).

reported and compared to the one for $x=0$.²⁰ One observes only a slight reduction of the saturation value of the local field at the muon and of T_c , while the temperature dependence is unaffected.

Above T_c the decay of the muon is conveniently described by a nearly static Kubo-Toyabe function. As in the pure compound the decay of the muon polarization can be conveniently fit using Keren analytical approximation,²¹ which yields reliable results in the fast fluctuating limit, namely, when $\tau_c \gamma_\mu \sqrt{\langle \Delta h^2 \rangle} \ll 1$, with τ_c the characteristic correlation time for the modulation of a magnetic field distribution of amplitude $\sqrt{\langle \Delta h^2 \rangle}$. At variance with $\text{Li}_2\text{VOSiO}_4$ in the Ti-doped samples one finds that $\tau_c \gamma_\mu \sqrt{\langle \Delta h^2 \rangle} \approx 1$. However,

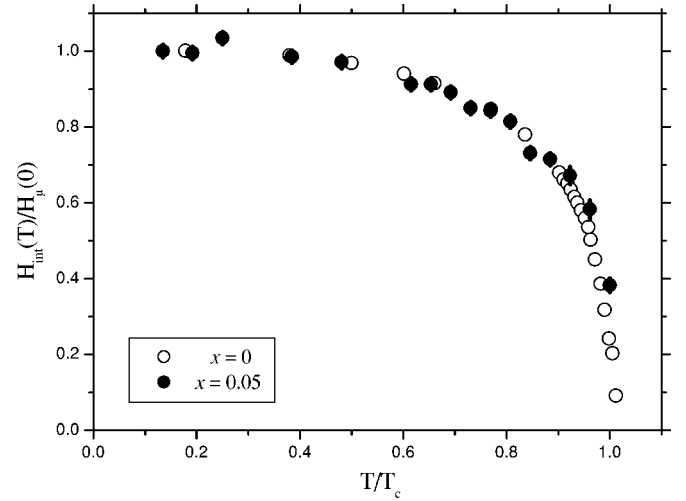


FIG. 6. Temperature dependence of the local field at the muon site H_{int} in $\text{Li}_2\text{V}_{1-x}\text{OTi}_x\text{SiO}_4$ for $x=0.05$, obtained from Eq. (2) in the text. Data for $\text{Li}_2\text{VOSiO}_4$ (from Ref. 20) are reported for comparison. Fields and temperatures are normalized by $H_{\text{int}}(0) = 309.2$ G and $T_c = 2.6$ K for $x=0.05$ and $H_{\text{int}}(0) = 313$ G and $T_c = 2.86$ K for $x=0$. For the $x=0.11$ a value for $H_{\text{int}}(0) = 297 \pm 5$ G was derived.

Keren approximation can still be used provided the fit is limited to a time $t \approx \tau_c$.²¹ In fact, the data above T_c were accurately fit up to $t = 6 \mu\text{s}$ with the function (Fig. 5)

$$A(t) = A(0) \exp(-\lambda t) P^K(H, \tau_c, \langle \Delta h^2 \rangle), \quad (3)$$

where the first term describes the spin-lattice relaxation driven by the fast fluctuations, while the second one is Keren analytical approximation of Kubo-Toyabe function. By fixing λ from the high longitudinal field measurements above 900 G and fitting μ SR data at different magnetic fields, the T dependence of τ_c was derived. It was found that τ_c , at variance with the pure compound where it diverges on cooling, is T independent and more than an order of magnitude larger (Fig. 7).

III. DISCUSSION

In the weak doping limit, when the so called “dilution model” should hold, the spin Hamiltonian of a 2DQHAF with only nearest-neighbor (NN) interactions can be written in the form

$$\mathcal{H} = J \sum_{i,j} p_i p_j \mathbf{S}_i \cdot \mathbf{S}_j = J(0) (1-x)^2 \sum_{i,j} \mathbf{S}_i \cdot \mathbf{S}_j, \quad (4)$$

where the $x=0$ Hamiltonian is modified simply by taking into account the probability p_i to find a spin at site i . This leads to a simple renormalization of the characteristic energy scales and the spin stiffness becomes²² $\rho_s(x) = \rho_s(0)(1-x)^2$. One can try to extend this result to frustrated 2DQHAF on a square lattice by considering that also a second-nearest-neighbor coupling is present. On qualitative grounds one would expect that, since both the probability to find a pair of nearest-neighbor spins and of next-nearest-neighbors scale as $(1-x)^2$, either J_1 or J_2 are renormalized by the same factor

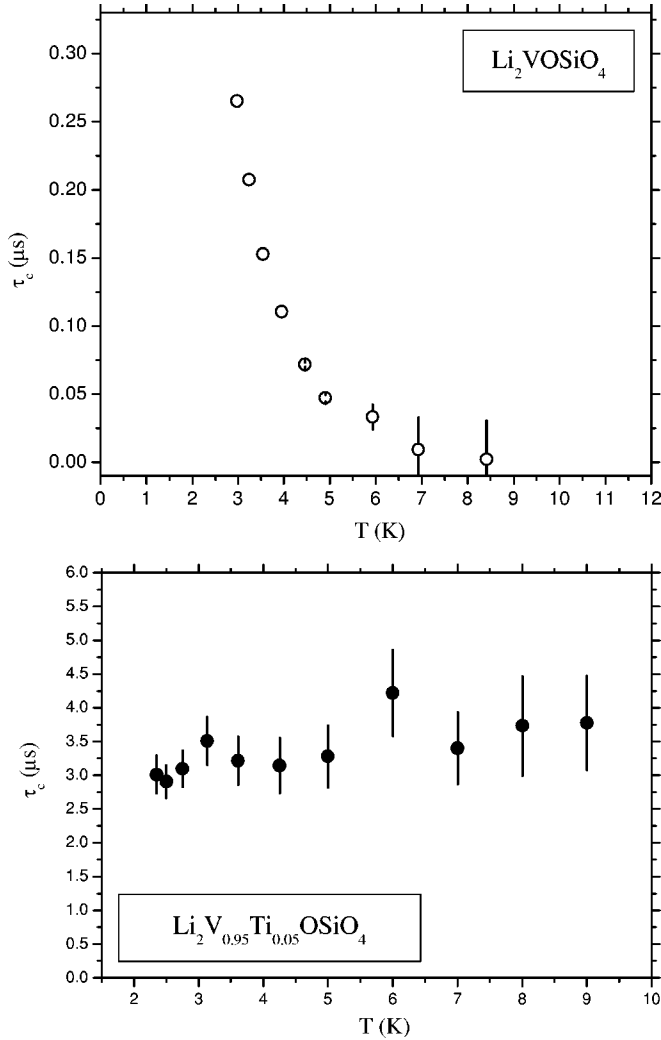


FIG. 7. Temperature dependence of the correlation time for the low frequency fluctuations in $\text{Li}_2\text{VOSiO}_4$ (top) and $\text{Li}_2\text{V}_{1-x}\text{OTi}_x\text{SiO}_4$ for $x=0.05$ (bottom).

and hence, the effective degree of frustration J_2/J_1 is unaffected by dilution. Moreover, the spin-stiffness is expected to scale as $(1-x)^2$ as for the nonfrustrated system. It will be shown hereafter that although the spin stiffness scales roughly as $(1-x)^2$ the experimental data evidence a modification of the effective J_2/J_1 ratio upon increasing x .

Preliminary information on the effects of spin dilution can be obtained from the analysis of the doping dependence of the transition temperature $T_c(x)$, which shows a different trend with respect to nonfrustrated 2DQHAF. In Fig. 2, $T_c(x)$, extracted either from susceptibility data or from the peak in ${}^7\text{Li } 1/T_1$, is shown. The initial suppression rate of T_c with Ti doping $-dT_c(x)/dx = CT_c(0)$, is not characterized by a C value close to the one theoretically predicted and experimentally found for nonfrustrated 2DQHAF, namely, $C \approx 3.2$.²³ In fact, in $\text{Li}_2\text{V}_{1-x}\text{Ti}_x\text{OSiO}_4$ $T_c(x)$ is rather well described by the expression $T_c(x) = T_c(0)(1-2x)$ (see Fig. 2), namely, by $C \approx 2$. This difference can be explained by resorting to the mean-field expression for $T_c(x)$ (Ref. 15)

$$k_B T_c(x) = J_\perp (1-x)^2 \xi(x, T_c)^2 \left(\frac{M(x)}{M(0)} \right)^2, \quad (5)$$

where $M(x)$ is the $T=0$ staggered magnetization, $\xi(x, T) \sim \exp[2\pi\rho_s(x)/T]$ the in-plane correlation length in lattice units² and J_\perp the interlayer coupling, which is reduced by a factor $(1-x)^2$ accounting for the probability to find two coupled spins in adjacent layers.

From this expression it is evident that the reduction of the staggered magnetization induced by dilution contributes to the reduction of $T_c(x)$. However, at variance with nonfrustrated compounds, in which a spin dilution of 5% was found to reduce the zero temperature magnetization already by about 9%,¹³ in $\text{Li}_2\text{V}_{1-x}\text{Ti}_x\text{OSiO}_4$ the same amount of doping reduces it only by 1% (see Fig. 6). This explains why in $\text{Li}_2\text{V}_{1-x}\text{Ti}_x\text{OSiO}_4$ the effect of doping on $T_c(x)$ is less pronounced. Moreover, it is observed that if in Eq. (5) one neglects the reduction of the staggered magnetization with doping and one considers that $\rho_s(x) \sim \rho_s(0)(1-x)^2$, one finds an initial suppression of $T_c(x)$ characterized by a coefficient $C=2$, exactly the one experimentally observed for $\text{Li}_2\text{V}_{1-x}\text{Ti}_x\text{OSiO}_4$. In the lower part of Fig. 2 the x dependence of the spin stiffness, estimated from Eq. (5) using the experimental values for $T_c(x)$ and neglecting the reduction with x of the staggered magnetization, is reported. It is observed that the spin stiffness is reduced by a factor $\approx (1-x)^2$ by spin dilution. A more accurate estimate of $\rho_s(x)$ can be done taking into account the reduction in $M(x)/M(0)$ estimated from the reduction of the local field at the muon for $T \rightarrow 0$ (Fig. 6). One finds that $\rho_s(x) \approx 1 - 1.5x$. Therefore the reduction of the spin stiffness with x is not exactly the one that one would obtain by rescaling J_1 and J_2 by the same factor $(1-x)^2$.

In this respect it is interesting to analyze the effect of Ti doping on the effective ratio between the competing exchange couplings. A first evidence that $J_2(x)/J_1(x)$ is not x independent comes from the analysis of the susceptibility data (see Fig. 2). The ratio between T_χ^m and the Curie-Weiss temperature Θ is a measure of the degree of frustration.²⁴ In fact, while for $J_2=0$ this ratio is close to unity, on increasing J_2 it diminishes, reaching a minimum for $J_2/J_1=0.5$ and then increases again.²⁴ In $\text{Li}_2\text{V}_{1-x}\text{Ti}_x\text{OSiO}_4$ this ratio is found to slightly decrease with x from $T_\chi^m/\Theta = 0.57 \pm 0.02$ for $x=0$ to $T_\chi^m/\Theta = 0.48 \pm 0.04$ for $x=0.11$. In principle, it is difficult to extract precise values of J_2/J_1 from the above ratios, however, if one considers that for small changes J_2/J_1 varies linearly with T_χ^m/Θ , the observed modifications imply a reduction in J_2/J_1 by 15–20% for $x=0.11$.

Also the analysis of the temperature dependence of the nuclear spin-lattice relaxation rate $1/T_1$ suggests that the effective ratio J_2/J_1 is affected by spin dilution. $1/T_1$ can be written in terms of the components of the dynamical structure factor $S(\mathbf{q}, \omega)$ at the nuclear Larmor frequency ω_L as

$$\frac{1}{T_1} = \frac{\gamma^2}{2N} \sum_{\mathbf{q}} |A_{\mathbf{q}}|^2 S(\mathbf{q}, \omega_L), \quad (6)$$

where γ is the nuclear gyromagnetic ratio and $|A_{\mathbf{q}}|^2$ is the form factor, which describes the hyperfine coupling of the

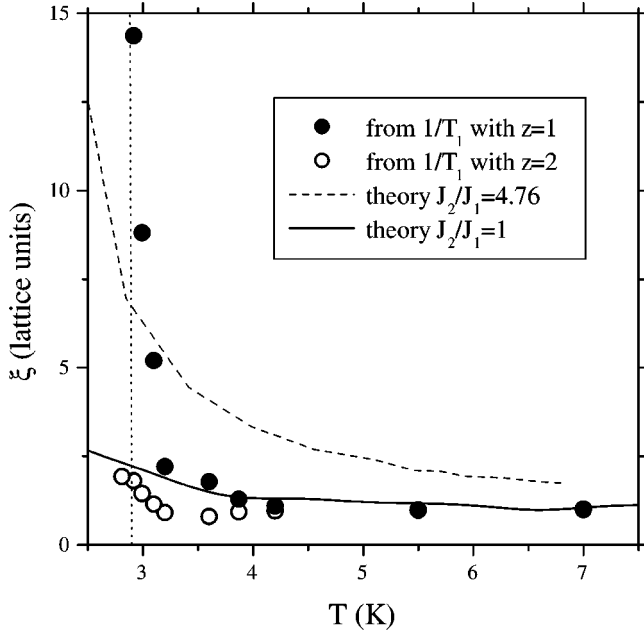


FIG. 8. Correlation length ξ extracted from ${}^7\text{Li}$ NMR $1/T_1$ in $\text{Li}_2\text{VOSiO}_4$ by inverting Eq. (7) in the text, in the assumptions that $z=1$ or that $z=2$. The data are compared with theoretical calculations, for different values of J_2/J_1 , made in the framework of pure-quantum self-consistent harmonic approximation (Ref. 26). The vertical dotted line indicates the transition to the collinear phase.

spin excitations at wave vector \mathbf{q} with the nuclei.

In nonfrustrated two-dimensional $S=1/2$ antiferromagnets it was pointed out that the in-plane correlation length can be conveniently derived from the nuclear spin-lattice relaxation rate.¹⁴ In fact, by applying scaling arguments for the amplitude and frequency of the collective spin excitations at wave vector \mathbf{q} , one can write the NMR relaxation rate in terms of the correlation length ξ as^{3,25}

$$\frac{1}{T_1} = C\varepsilon\xi^{\varepsilon+2}\frac{\beta^2\sqrt{2\pi}}{\omega_E}\left(\frac{1}{4\pi^2}\right)\int_{\text{BZ}}d\mathbf{q}\frac{|A_{\mathbf{q}}|^2}{(1+q^2\xi^2)^2}, \quad (7)$$

where $C=\gamma^2S(S+1)/3$, z is the dynamical scaling exponent [for $J_2/J_1=0$ $z\approx 1$ (Ref. 14)], ε is a coefficient accounting for the reduction of the amplitude of spin excitations due to quantum fluctuations, $\omega_E\sim\sqrt{J_1^2+J_2^2}k_B/\hbar$ is the Heisenberg frequency,⁷ describing the uncorrelated spin fluctuation for $T\rightarrow\infty$, and β is a normalization factor which preserves the spin sum rule. The form factors have been calculated on the basis of the hyperfine constants determined for the pure $\text{Li}_2\text{VOSiO}_4$.^{6,7}

Once z is defined a one-to-one relationship between T_1 and ξ is established, and one can determine ξ from ${}^7\text{Li}$ $1/T_1$. Then one can compare these results for ξ with the recent theoretical predictions for the temperature dependence of ξ , for different values of J_2/J_1 , based on the pure-quantum self-consistent harmonic approximation.²⁶ In Fig. 8 ξ extracted from ${}^7\text{Li}$ NMR relaxation data in $\text{Li}_2\text{VOSiO}_4$ are reported both in the assumptions that $z=1$ or that $z=2$.

One observes that, above the crossover from 2D to 3D yielding the divergence of $1/T_1$ at T_c , ξ data derived for z

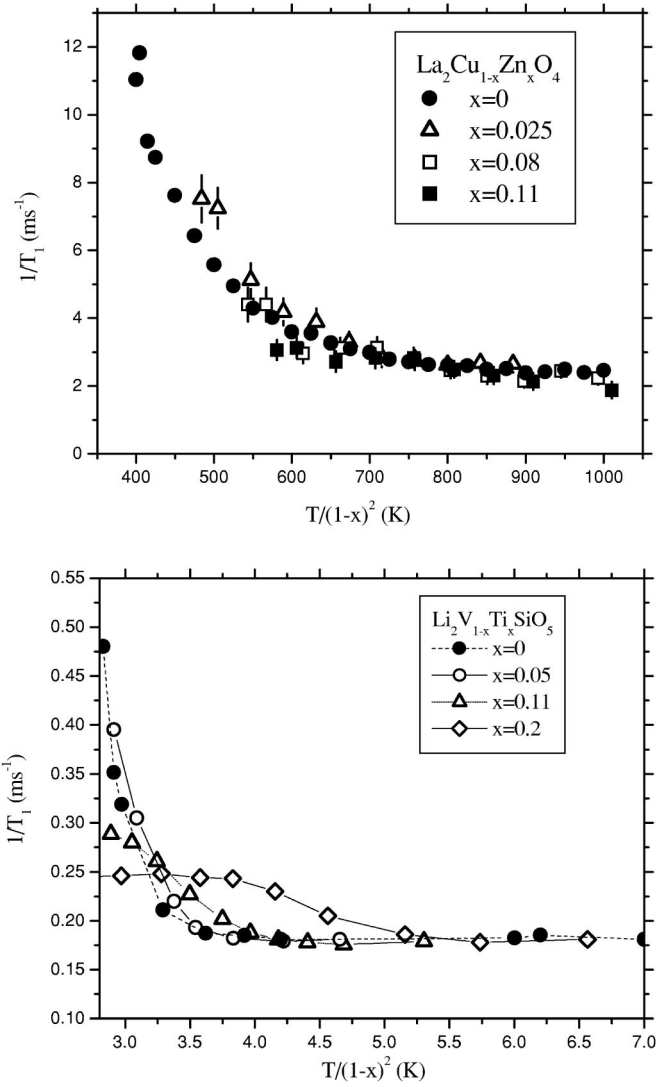


FIG. 9. Comparison of ${}^{63}\text{Cu}$ $1/T_1$ in $\text{La}_2\text{Cu}_{1-x}\text{Zn}_x\text{O}_4$ and ${}^7\text{Li}$ $1/T_1$ in $\text{Li}_2\text{V}_{1-x}\text{OTi}_x\text{SiO}_4$ as a function of the scaled temperature $T/(1-x)^2$.

$=1$ are in rather good agreement with the theoretical calculations for $J_2/J_1=1$. Larger ratios of J_2/J_1 and a dynamical scaling exponent $z=2$ do not appear to be consistent with the experimental findings. This suggests that the same scaling laws used for pure 2DQHAF could still be valid in the presence of frustration. For $z=1$ and $T\ll J_1+J_2$, if the form factor is weakly q dependent as for ${}^7\text{Li}$ in $\text{Li}_2\text{VOSiO}_4$, one has that^{2,14}

$$\frac{1}{T_1} \sim \xi \sim \exp[2\pi\rho_s(x)/T]. \quad (8)$$

Then, if J_1 and J_2 are reduced to the same extent by dilution and $\rho_s(x)=\rho_s(0)(1-x)^2$, the T dependence of $1/T_1$ data should be x independent once the temperature is rescaled to $T/(1-x)^2$. In fact, in diluted nonfrustrated 2DQHAF as $\text{La}_2\text{Cu}_{1-x}\text{Zn}_x\text{O}_4$, such a scaling does occur (see Fig. 9). On the other hand, in the diluted frustrated 2DQHAF $\text{Li}_2\text{V}_{1-x}\text{Ti}_x\text{OSiO}_4$, such scaling does not seem to be accurate

any longer, suggesting that also the effective ratio J_2/J_1 is changing. In fact, one has to observe that while the spin Hamiltonian for a diluted nonfrustrated 2DQHAF on a square lattice can still be mapped onto the same Hamiltonian, provided the exchange coupling is renormalized, the spin Hamiltonian for the frustrated 2DQHAF on a square lattice can no longer be mapped onto the same Hamiltonian as dilution in the J_2 - J_1 model yields the appearance of triangular spin configurations.

After having presented these arguments suggesting a variation of the effective ratio $J_2(x)/J_1(x)$ and a negligible reduction of $M(x)$, the effect of spin vacancies on the distortion initially observed in undoped frustrated systems will be discussed.⁶ As pointed out in the Introduction, $\text{Li}_2\text{VOSiO}_4$ is characterized by $J_2/J_1 > 0.8$ and hence by a twofold degenerate collinear ground state, with a magnetic wave vector which can be either $\mathbf{Q}=(0, \pi/a)$ or $\mathbf{Q}=(\pi/a, 0)$. At low- T , after an Ising transition, the spin system will eventually collapse in either one of the two collinear ground states.^{10,27} Now, in a real system a finite spin-lattice coupling exists and for $J_2/J_1 > 0.8$ it would favor a tetragonal to orthorhombic distortion.²⁸ In fact, the behavior of ^{29}Si NMR spectra and $1/T_1$ observed in some $\text{Li}_2\text{VOSiO}_4$ samples is consistent with such a distortion.⁷ ^{29}Si form factor $|A_{\vec{q}}|^2$ is peaked at $(q_x = \pi/a, q_y = \pi/a)$ and vanishes at the critical wave vector $\mathbf{Q}=(0, \pi/a)$ or $\mathbf{Q}=(\pi/a, 0)$. Hence, on approaching T_c , as the spectral weight shifts to the critical wave vector of the envisaged *collinear* order, $1/T_1$ should decrease and no peak observed. However, in the pure $\text{Li}_2\text{VOSiO}_4$ a peak in $1/T_1$ was observed suggesting that a distortion modifying ^{29}Si form factor takes place.^{6,7} In Ti-doped samples (Fig. 4) no peak in ^{29}Si $1/T_1$ is observed at T_c , pointing out that Ti impurities tend to hinder this distortion.

Finally, we point out that above T_c Ti doping also hinders the very-low-frequency dynamics evidenced by μSR measurements in $\text{Li}_2\text{VOSiO}_4$ (Fig. 7).²⁰ These dynamics were associated with the motion of domain walls separating re-

gions were correlations with $\mathbf{Q}=(0, \pi/a)$ or $\mathbf{Q}=(\pi/a, 0)$ develop before the lattice distortion removes their degeneracy. Although a clear explanation of such a phenomenon goes beyond the aim of the present work, the observation of a T independent much longer correlation time measured by μSR suggests that Ti impurities might pin the motions of domain walls.

IV. CONCLUSIONS

In conclusion, a throughout investigation of a spin diluted frustrated 2DQHAF system by means of NMR, μSR , and susceptibility measurements has been presented. It has been shown that the decrease of the magnetic ordering temperature is consistent with a reduction of the spin stiffness by a factor $\simeq(1-x)^2$ and with a minor effect of spin dilution on the sublattice magnetization. The analysis of the magnetic susceptibility and of the nuclear spin-lattice relaxation rate shows that the effective ratio $J_2(x)/J_1(x)$ decreases with x , namely, that the two coupling constants are not renormalized in the same way by dilution. This would actually mean that the spin Hamiltonian of a frustrated 2DQHAF on a square lattice cannot be mapped onto the same square-lattice Hamiltonian after spin dilution has occurred. Finally it was shown that the low frequency dynamics observed in pure $\text{Li}_2\text{VOSiO}_4$ by means of μSR measurements disappears in $\text{Li}_2\text{V}_{1-x}\text{Ti}_x\text{OSiO}_4$. Moreover the absence of a peak in ^{29}Si NMR relaxation rate at the transition indicates that the distortion induced by frustration might be hindered by doping.

ACKNOWLEDGMENTS

We would like to thank A. Fubini for sending us the results of the theoretical calculations reported in Ref. 26, and T. Roscilde for useful discussions. This work was supported by PRIN2004 National Project ‘‘Strongly Correlated Electron Systems with Competing Interactions.’’

¹See, for example, E. Dagotto and T. M. Rice, *Science* **271**, 619 (1995); E. Dagotto, *Rep. Prog. Phys.* **62**, 1525 (1999), and references therein
²S. Chakravarty, B. I. Halperin, and D. R. Nelson, *Phys. Rev. B* **39**, 2344 (1989).
³A. Rigamonti, F. Borsa, and P. Carretta, *Rep. Prog. Phys.* **61**, 1367 (1998).
⁴O. P. Vajk, P. K. Mang, M. Greven, P. M. Gehring, and J. W. Lynn, *Science* **295**, 1691 (2002).
⁵P. Chandra and B. Doucot, *Phys. Rev. B* **38**, 9335 (1988).
⁶R. Melzi, P. Carretta, A. Lascialfari, M. Mambri, M. Troyer, P. Millet, and F. Mila, *Phys. Rev. Lett.* **85**, 1318 (2000).
⁷R. Melzi, S. Aldrovandi, F. Tedoldi, P. Carretta, P. Millet, and F. Mila, *Phys. Rev. B* **64**, 024409 (2001).
⁸P. Carretta, N. Papinutto, R. Melzi, P. Millet, S. Gouthier, P. Mendels, and P. Wzietek, *J. Phys.: Condens. Matter* **16**, S849 (2004).
⁹A. Bombardi, J. Rodriguez-Carvajal, S. Di Matteo, F. de Bergevin, L. Paolasini, P. Carretta, P. Millet, and R. Caciuffo, *Phys.*

Rev. Lett. **93**, 027202 (2004).

¹⁰P. Chandra, P. Coleman, and A. I. Larkin, *Phys. Rev. Lett.* **64**, 88 (1990).
¹¹H. J. Schulz and T. A. L. Ziman, *Europhys. Lett.* **18**, 355 (1992); H. J. Schulz, T. A. L. Ziman, and D. Poilblanc, *J. Phys. I* **6**, 675 (1996).
¹²B. Keimer, N. Belk, R. J. Birgeneau, A. Cassanho, C. Y. Chen, M. Greven, M. A. Kastner, A. Aharony, Y. Endoh, R. W. Erwin, and G. Shirane, *Phys. Rev. B* **46**, 14 034 (1992).
¹³M. Corti, A. Rigamonti, F. Tabak, P. Carretta, F. Licci, and L. Raffo, *Phys. Rev. B* **52**, 4226 (1995).
¹⁴P. Carretta, A. Rigamonti, and R. Sala, *Phys. Rev. B* **55**, 3734 (1997).
¹⁵Yu-Chang Chen and A. H. Castro Neto, *Phys. Rev. B* **61**, R3772 (2000); A. L. Chernyshev, Y. C. Chen, and A. H. Castro Neto, *Phys. Rev. B* **65**, 104407 (2002).
¹⁶While for a two-dimensional square-lattice the percolation threshold for site dilution is $x \simeq 0.41$, preliminary estimates carried out

- by T. Roscilde show that in the presence of next-nearest-neighbor couplings along the diagonals the percolation threshold increases to $x=0.5928(1)$.
- ¹⁷P. Millet and C. Satto, *Mater. Res. Bull.* **33**, 1339 (1998).
- ¹⁸R. D. Shannon, *Acta Crystallogr., Sect. A: Cryst. Phys., Diffr., Theor. Gen. Crystallogr.* **32**, 751 (1976).
- ¹⁹S. T. Ting, P. Pernambuco-Wise, J. E. Crow, E. Manousakis, and J. Weaver, *Phys. Rev. B* **46**, 11 772 (1992).
- ²⁰P. Carretta, R. Melzi, N. Papinutto, and P. Millet, *Phys. Rev. Lett.* **88**, 047601 (2002).
- ²¹A. Keren, *Phys. Rev. B* **50**, 10 039 (1994).
- ²²See, for example, A. W. Sandvik, *Phys. Rev. B* **66**, 024418 (2002), and references therein.
- ²³A. R. McGurn, *J. Phys. C* **12**, 3523 (1979).
- ²⁴S. Bacci, E. Gagliano, and E. Dagotto, *Phys. Rev. B* **44**, 285 (1991); R. R. P. Singh and R. Narayanan, *Phys. Rev. Lett.* **65**, 1072 (1990); G. Misguich, B. Bernu, and L. Pierre, *Phys. Rev. B* **68**, 113409 (2003).
- ²⁵A. Rigamonti, P. Carretta, and N. Papinutto, in *Correlated Spin Dynamics and Phase Transitions in Pure and in Disordered 2D $S=1/2$ Antiferromagnets from NMR-NQR* (Springer-Verlag, Berlin, 2005).
- ²⁶L. Capriotti, A. Fubini, T. Roscilde, and V. Tognetti, *Phys. Rev. Lett.* **92**, 157202 (2004).
- ²⁷C. Weber, L. Capriotti, G. Misguich, F. Becca, M. Elhajal, and F. Mila, *Phys. Rev. Lett.* **91**, 177202 (2003).
- ²⁸F. Becca and F. Mila, *Phys. Rev. Lett.* **89**, 037204 (2002).